Inflatable-Rigidizable Solar Concentrators for Space Power Applications

Frederick H. Redell, [*] Justin Kleber, [†] David Lichodziejewski[‡]
L'Garde, Inc., Tustin, California 92780

and

Dr. Gyula Greschik[§]
University of Colorado at Boulder, Boulder, Colorado 80309

This paper summarizes the development of L'Garde's Long Lived Solar Concentrator technology which utilizes material rigidization methods to provide a long lasting reflector shape without requiring continuous inflation. Material studies were conducted and testing completed on 1 m reflectors to down select work-hardening of an aluminum/plastic laminate as the rigidization method of choice over cold rigidization of a Kevlar®/thermoplastic-elastomer composite. The results of the surface measurements are summarized showing slope errors as low as 12 milliradian and a focal dot with a radius as small as 37 mm. Two 3-m reflectors were constructed with one tested by photogrammetry and the results compiled while the second is packaged for future testing at NASA Glenn's Tank 6 Solar Simulator facility. Significant sciential data were collected through testing which showed that even when subjected to 1 g earth loading conditions, the shape of the reflector could be maintained allowing for future ground testing of the concept. The result is an advanced concept poised for continued development.

The results of a system study using this technology are summarized and give guidance to properly sizing and positioning the reflector system on a spacecraft. The heart of this technology advancement resides in its mission enabling capability. This technology advancement diminishes two hurdles for large power concentration. First, rigid mirror reflectors require large spaces to stow thereby limiting the aperture size of the concentrator. Second, purely inflatable reflectors will require some make-up gas to remain inflated in space subsequently limiting the mission lifetime.

Lastly, a novel approach to remove the reflector canopy, further improving the performance of the reflector, was developed and tested on the 3 m reflector. This would remove the transmission losses that would occur when collecting the solar energy and remove the need to find a canopy material that wouldn't darken over the life of the reflector system.

Nomenclature

$\underline{\underline{S}}$	=	shear on an element
$\underline{\underline{C}}$	=	stress on an element
$tr(\underline{\underline{C}})$	=	trace operator (Sum of the diagonal elements of a square matrix)
F/D	=	ratio of focal distance of parabola to diameter
σ_θ	=	stress in the horizon direction
σ_ϕ	=	stress in the meridional direction
S_θ	=	shear in the horizon direction

[*] Staff Engineer, fred@lgarde.com, AIAA Member.
[†] Staff Engineer, justin@lgarde.com, AIAA Member.
[‡] Principal Investigator, leo@lgarde.com, AIAA Member.
[§] Research Associate, greschik@Colorado.EDU, AIAA Member.

S_ϕ = shear in the meridional direction
E_{eff} = effective modulus
E_{warm} = modulus at warm temperature
E_{cold} = modulus at cold temperature
T_g = glass transition temperature

I. Introduction

Inflatable-rigidizable structures have generated significant interest recently as enablers for space missions where mass, stowed volume, lifetime, and system cost are driving factors for mission feasibility. As the technology leader in inflatable space structures, L'Garde has advanced the technology to include inflatable-rigidizable structures.

Using an inflatable reflector as the core of a solar concentrator provides a superior solution over conventional reflector dishes because the inflatable reflector has significantly lower mass and stowed volume. The ability to rigidize the reflector following inflation and shaping greatly increases the superiority of the inflatable reflector design by eliminating the need to carry make-up gas to maintain the proper inflation pressure and reflector shape. Inflation gas is needed only to shape the reflector, which would be made of a rigidizable material. Because the rigidized reflector is capable of accurately holding its shape without pressure, the lifetime of the concentrator is extended, and it can be used to provide solar propulsion, to provide thermal energy to a dynamic converter, and to illuminate a solar array or other energy conversion device. Combining all these functions into one subsystem presents a dramatic reduction in cost for deep space missions. Furthermore, the canopy can be removed and discarded; thereby improving the efficiency of the concentrator. Fig. 1[1,2] shows an off-axis, inflatable-rigidizable concentrator.

L'Garde has done extensive research and testing of rigidizable materials including gel-impregnated fabrics, epoxy-coated fabrics, UV-curable fabrics, and thermosetting polymer composites. All these materials demonstrated surface degradation due to dimensional changes of the material during curing. However, two rigidizable materials that have shown tremendous potential for this application are aluminum/plastic laminates, and Kevlar®/thermoplastic elastomer composites.

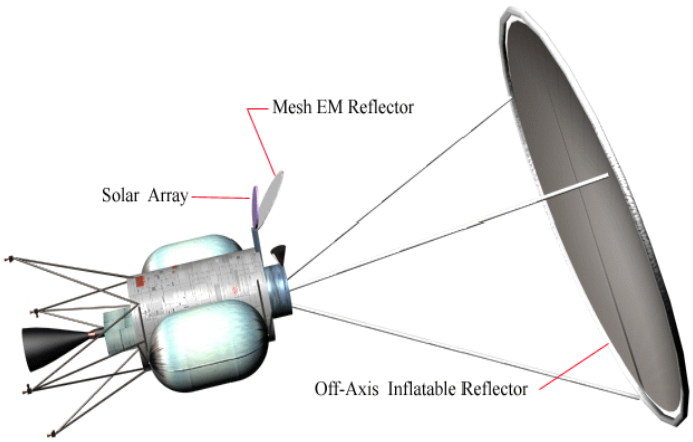

Figure 1. Inflatable-Rigidizable Concentrator for Deep Space Missions.

Aluminum/plastic laminates are made of aluminum foil and thin plastic films that are combined into thin, packagable membranes. A structure that uses such a membrane is inflated to a pressure that stretches the membrane to a point where the plastic stays in its elastic region, but the aluminum enters its plastic region. The aluminum is work-hardened and forms a stiff shell, which is capable of retaining its shape and carrying loads after the inflation pressure is released. Aluminum/plastic laminates were used successfully by L'Garde on the Echo balloons and several inflatable satellites, including a 3.7 meter sphere launched for the Air Force Research Laboratory (AFRL).[3]

The Kevlar®/thermoplastic elastomer composite membrane is rigidized by cooling the membrane below the glass transition temperature (T_g) of the thermoplastic elastomer; thereby stiffening the material. This differs significantly from other composite approaches because no chemical reaction occurs. By utilizing metalized plastic surfaces, the material could potentially be used in specular applications requiring highly accurate reflective surfaces. A similar composite was used by L'Garde in a rigidizable space truss, which withstood over 2.2 kN of compression load, yet had a mass of only 3.86 kg.[4]

L'Garde chose the aluminum/plastic laminate and Kevlar®/thermoplastic elastomer composite as the candidate materials of the Long-Lived Solar Concentrator program. The authors conducted extensive research and tests to

characterize the performance of the materials, and further develop their applications for advanced inflatable-rigidizable solar concentrator designs.

II. Reflector Design and Analysis

A. Basic Reflector Design

L'Garde has a series of unique tools developed over many programs to design the precise gore shapes necessary for reflector fabrication. Initially a code called FLATE is utilized which calculates the gore shapes given the geometric requirements and material properties. This code can compensate for the seams required at the edges of the gores to bond them together. Another tool called FAIM is utilized to predict the inflated shape given the flat gore shape. Using these tools, a study was conducted using the aluminum laminate material properties to calculate the optimum number of gores required for the reflector design. The results of this study are shown in Fig. 2. The plot shows the predicted reflector precision as a function of the number of gores. As expected, analytically, the reflector precision improves with a greater number of gores. However, in reality, manufacturing errors are introduced at the seams and experience shows that the best compromise is to select the least number of gores that achieves a good predicted RMS accuracy; in this case we have selected the 12 gore design. It should be noted that the gore number optimization was conducted using a specific aluminum/plastic laminate. However, the same number of gores was used to fabricate all the Phase II 1 m test articles since the results are roughly the same. Separate gore shapes were used based on the material properties but the number of gores was held constant. This allowed for leveling the manufacturing errors in the experiments and increasing the sensitivity of the material choice to the results.

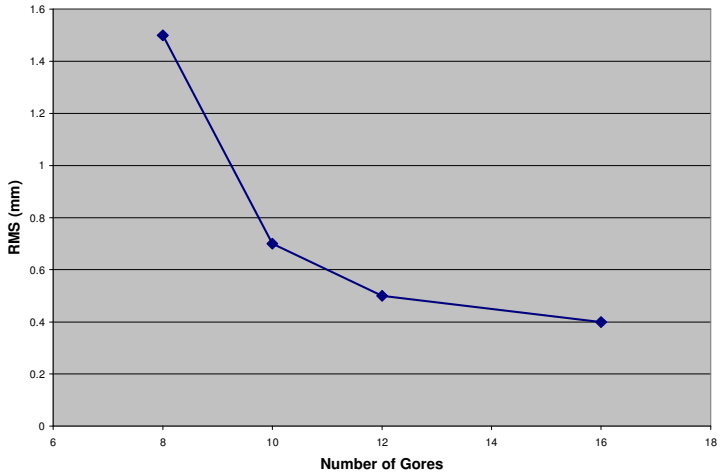

Figure 2. Gore Optimization Study Results for a 1-meter Reflector..

A flat gore design from FLATE/FAIM based on the above analysis is then generated. A high precision template of this pattern is fabricated for aluminum test articles while the Kevlar® composites are cut with our gore cutting laser table. The gores are seamed together at butt joints along the edges using seams. The finished reflector is then ring-mounted and tested.

B. Structural Analysis

In addition to the analyses performed to understand the material selection, a variety of analyses were performed to better understand the material shaping during pressurization and release. Consider that plastification is governed by shear and in the 3D context the deviatoric stress tensor is:

$$\underline{\underline{S}} = \underline{\underline{C}} - \frac{1}{3} tr(\underline{\underline{C}}) \tag{1}$$

The deviatoric stress tensor is the stress that contributes to shear (explicitly it is the stress on an element minus the hydrostatic component). It is generally acceptable to assume associated flow, which is that the plastic deformations are work-proportional to the governing deviatoric stresses. Applying this to two key examples can show interesting results; these examples are the case of a pressurized tube and sphere.

In a sphere the stress occurs equally in both directions of the surface (by geometry):

$$\underline{\underline{C}} = \begin{bmatrix} \sigma & 0 & 0 \\ 0 & \sigma & 0 \\ 0 & 0 & 0 \end{bmatrix}, \tag{2}$$

therefore,

$$\underline{\underline{S}} = \begin{bmatrix} \sigma/3 & 0 & 0 \\ 0 & \sigma/3 & 0 \\ 0 & 0 & -2\sigma/3 \end{bmatrix}. \tag{3}$$

Thus equal plastic deformation occurs in both in-surface directions and some in the direction through the surface. While in a pressurized tube the stress in the longitudinal direction is twice that of the hoop direction (by geometry):

$$\underline{\underline{C}} = \begin{bmatrix} \sigma & 0 & 0 \\ 0 & \sigma/2 & 0 \\ 0 & 0 & 0 \end{bmatrix}, \tag{4}$$

therefore,

$$\underline{\underline{S}} = \begin{bmatrix} \sigma/2 & 0 & 0 \\ 0 & 0 & 0 \\ 0 & 0 & -\sigma/2 \end{bmatrix}, \tag{5}$$

resulting in no longitudinal plastic deformation. The geometries of the sphere and the tube bound the geometry of the paraboloid where for large F/D the shape approaches a sphere and for very small F/D the shape approaches a tube. Therefore, since the stress in each direction depends upon the F/D, a different amount of shear will occur in each direction and thus a different amount of plastic deformation. See Table 1.

Table 1. Stress and Deviatoric Stress Ratios in Reflector as a Function of F/D.

F/D	$\sigma_\theta/\sigma_\phi$ at edge	S_θ/S_ϕ at edge
0.5	1.20	1.75
1.0	1.06	1.19
1.5	1.02	1.06

Adding to the directional deformation differences due to the parabolic shape is the physical method used to assemble the reflector. This is done by creating flat gores that are seamed together to form a discrete curved shape in the horizon direction (for a on-axis reflector 4-gore = square, 6-gore = hexagon, 10-gore = octagon…infinite-gore = circle) with a shallower than final shape at the seams in the meridian direction. When inflated the gore center needs to shape more in the horizon direction while the seams shape more in the meridian direction. This example can be likened to a parachute where the gores are the billowing areas and the seams are the cords. This leads to differential straining, which results in non-uniform rebounding of the reflector after rigidization. This can contribute to non-uniform rebounding.

Having the directional deformation differences coupled with the method of assembly results in more circumferential strain in the gore area while more meridian strain occurs in the seams. This creates a slack in the gores and thus a buckling of the excess material when pressure is released could occur. To combat this, specific laminates were tested as describe in the material section of this report.

C. Gore Shaping

The structural work included deriving a method to use the material's mechanical property results in our current software (FAIM and FLATE). The following was derived to accomplish this.

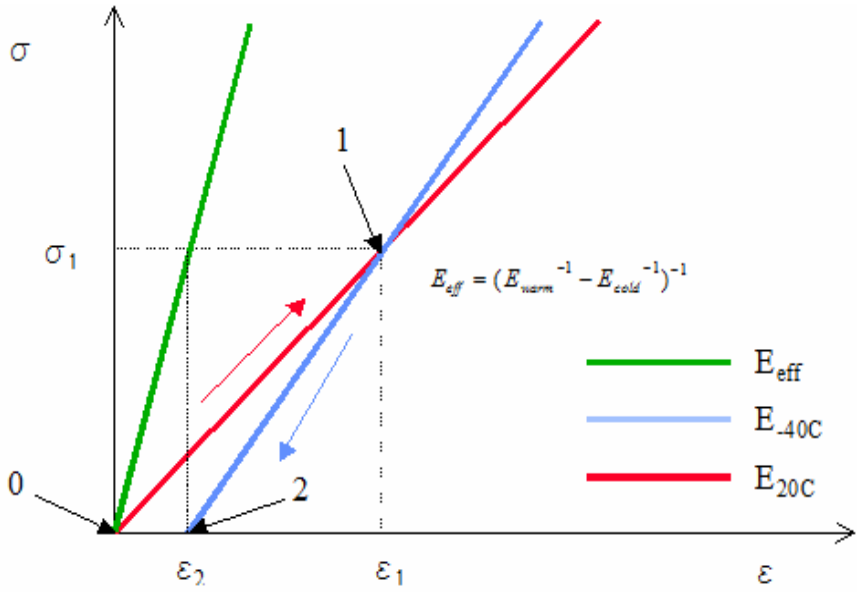

Figure 3. Diagram for Determining Sub-T_g Material Properties for Gore Shape Analysis.

Description of the process of cold rigidization method material properties as shown in Fig. 3:

- Start un-pressurized at point 0.
- Pressurize while warm to point 1, the reflector is strained past the target shape.
- Hold at pressure and cool reflector, the reflector's modulus of elasticity changes as the material stiffens.
- Remove pressure and reflector rebounds to point 2, the final shape is then dictated by the strain at point 2.
- Reflector is at final shape, rigid and ready for use.

The effective modulus is defined by the line that extends from the origin and intersects the point where the final stress intersects the film stress. This methodology allows us to use our current modeling tools (FAIM and FLATE) with linear material properties to analyze the gore shape using the effective modulus defined by the warm and cold properties of the laminate. The resulting effective modulus is independent of the final stress and assumes the material is below the yield point (which is a good assumption for our Kevlar® composite).

To fully understand the shaping that occurs with the aluminum laminate a similar method was used that involves the yielding of the aluminum laminate. The aluminum is pressurized up along the linear-elastic region of the stress-strain curve and continues above the yield limit. Once the reflector is at full pressure, the pressure is released and the rebound occurs along a line that is parallel to the linear-elastic region but is offset due to yielding. The result is similar to the cold rigidizable where an amount of strain is retained in the material at point 2. This method has some dependence on the film stress, which makes the final shape more difficult to achieve for unfavorable F/D ratios. This subject should be analyzed with codes that account for the material properties directly for future investigations.

III. Materials Selection

The two techniques that were under consideration for space rigidization of the parabolic reflector are work hardening of an aluminum/plastic laminate (aluminum laminate concept) and cold rigidization of a Kevlar®/thermoplastic-elastomer composite (sub-T_g concept). To test these techniques a series of reflectors were built and tested for surface accuracy and slope error. The goal of the investigation was to shed light on the difficulties encountered during the first phase and discover a path to improve the technology. A list of the material difficulties included:

- Coefficient of Thermal Expansion (CTE) of the sub-T_g concept: This was a primary concern for the sub-T_g concept due to the high CTE of the material. Since the material shrinks as it becomes cool and cooling the material rigidizes it, the shape of the reflector was hard to manage. Additionally, since the material is cold rigidized, thermal transients on orbit would create distortions in the reflector shape.

- Dynamic Rebound of the Aluminum Laminate: This was a primary concern for the aluminum laminate after experimental observations were made. This difficulty could be due to the material or alleviated by the material. After rigidization and depressurization, small areas of material near the edges of the reflectors would "pop" and reverse in curvature. This occurred just after the pressure was released and for a few seconds thereafter. The popping occurred near the outer diameter of the reflector on the flattest or least doubly curved regions. This distortion never occurred inside the inner half of the diameter, the most doubly curved section of the reflector.

In an attempt to alleviate these difficulties, material selections were made for each technology and tested.

IV. Canopy Release

A reflector that has been rigidized after inflation and shaping no longer needs a canopy to provide an enclosed chamber for inflation. Thus, the canopy can be discarded after rigidization, subsequently eliminating transmission losses upon collection and reflection back to the secondary collector. This would provide an increase in collector efficiency versus non-rigidized, continuously-inflated reflectors.

The biggest challenge in removing the canopy in a gossamer reflector is in ensuring that there is negligible load applied to the structure and reflector while removing and discarding the canopy. Several methods for canopy removal were considered here; two were selected for further development. The first method employed a tear strip that mechanically separated the canopy from the reflector around the perimeter by ripping thru several thin layers of plastic film, which were stacked upon one another. This concept was modeled after tear strips used in consumer product applications, such as chewing gum wrappers. The second method used voltage-release epoxy adhesive. Here, the adhesive is used to bond the canopy to the reflector with a high-strength bond. After inflation, voltage is applied across the bond, which causes the adhesive to lose its adhesive strength, thereby allowing for virtually load-free separation of the canopy from the reflector. The canopy was bonded to the reflector in such a way that the bond was in shear during inflation, and in peel during removal This further contributed to a virtually load-free condition.

Based upon the results of the experiments, the method that relied on the voltage-release adhesive as the separation mechanism was chosen as the favored method for canopy removal. This method was used with success on one of the 3-meter test articles, which will be discussed in more depth later.

V. System Study

In order to characterize a generic, off-axis solar concentrator that features inflatable-rigidizable technology, a simplified model of such a system was created. For simplicity, one concentrator assembly was modeled with nominal spacecraft loading conditions applied. The model only included the concentrator assembly outboard of the spacecraft, and included the inflation system. The goal of this study was to determine a reasonable indication of the physical characteristics of a rigidizable concentrator assembly, and to identify parts of the system that would benefit from further development. Table 2 shows a summary of the results of the system model.

The study indicated that a rigidizable concentrator would have greater mass than a continuously-inflated, thin-film system. This is to be expected; however, this would be offset somewhat by the fact that no make-up gas is needed on the spacecraft to maintain proper inflation pressures. Table 3 presents a mass breakdown of the system components. These results were not surprising considering that the reflector material would need to be considerably thicker in order to form and maintain the shape of the reflector. Furthermore, a more substantial support structure – the torus and struts – would need to be used to support the high loads generated during rigidization. In fact, the torus represents the highest percentage of the system mass, and, therefore, presents the best opportunity for mass savings.

Table 2. System Model Summary.

CONFIG.	MASS (Kg)	STOWED VOLUME (m^3)	SPECIFIC POWER (W/Kg)	AREA POWER DENSITY (W/m^2)	NATURAL FREQUENCY (Hz)
1	94	2.4	654	457	8.6
2	95	2.0	736	495	12.6
3	100	2.0	745	514	10.2
4	103	2.1	751	527	7.7

Table 3. System Model Mass Breakdown.

COMPONENT	MASS (kg)				PERCENTAGE OF TOTAL MASS			
Configuration No.	**1**	**2**	**3**	**4**	**1**	**2**	**3**	**4**
Reflector	10	10.5	11	11	10.7	11.1	11	10.7
Canopy	3.1	3.3	3.6	3.6	3.4	3.5	3.6	3.5
Torus and Connectors	61.4	55.2	54.1	52.9	65.4	58.0	54.0	51.0
Rear Strut	2.4	3.3	4.2	5.0	2.7	3.5	4.2	4.9
Front Struts (2X)	4.4	7.6	9.7	11.4	9.5	16	19.4	22.1
Inflation System	7.8	7.5	7.8	8.0	8.3	7.9	7.8	7.8

VI. Experimental Results

A. 1-Meter Test Reflectors

Several experiments have been conducted on 1-meter test articles with promising results. To analyze the performance of the reflectors, photogrammetry was used along with slope error and raytracing codes developed by the authors. Only macroscopic surface errors are considered in these calculations, since microscopic surface roughness of the reflector surface was not the prime focus of this study. Photos of aluminum and sub-T_g test articles (left and right respectively) are shown Fig. 4. A summary of calculated results is shown in Table 4.

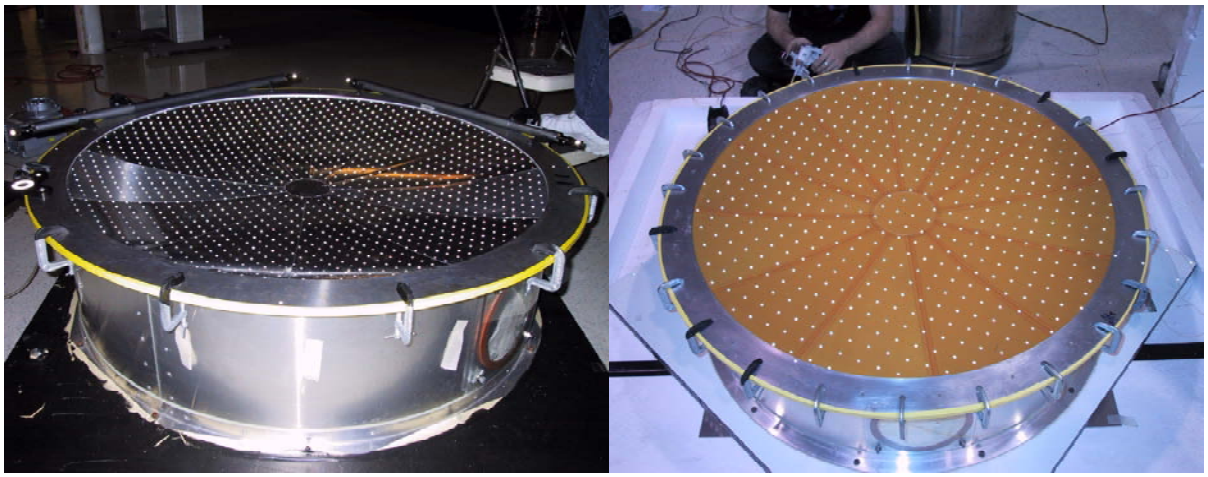

Figure 4. 1-Meter Test Articles.

From the data in Table 4, it is apparent that the aluminum reflectors currently perform much better. The sub-Tg reflectors also perform well but would require more research to arrive at a suitable candidate. Shown in Fig. 5 and Fig. 6 are typical collection plots from the sub-Tg and aluminum reflector tests. It can be seen from these plots that the aluminum reflector holds the correct shape much better than the sub-Tg reflectors. Subsequently, the aluminum

reflector technology has been down selected for the 3 m test articles. Additionally, the aluminum reflectors would most likely result in a lower overall system mass, provide a clearer path to using even thinner materials, and have a easily-managed surface. This is due to the aluminum being thinner allowing smaller structural components and a smaller inflation system to be used. These and other system characteristics will be studied further in the system design task.

Table 4. 1-Meter Test Article Results.

			Rigid				Rigid	Re-Rigidized
Sub Tg	Reflector 1	RMS Surface Error (mm)	0.91	Aluminum	Reflector 4	RMS Surface Error (mm)	0.47	0.49
		RMS Slope Error (mRadian)	27.7			RMS Slope Error (mRadian)	14.4	12.2
		Focus (m)	0.89			Focus (m)	0.93	0.89
		RMS Focal Position Error (mm)	54.38			RMS Focal Position Error (mm)	29.55	24.24
		90% Focal Circle Radius (mm)	88.67			90% Focal Circle Radius (mm)	45.59	36.88
	Reflector 2	RMS Surface Error (RMS)	0.90		Reflector 5	RMS Surface Error (mm)	0.47	0.51
		RMS Slope Error (mRadian)	33.30			RMS Slope Error (mRadian)	13.7	12
		Focus (m)	0.90			Focus (m)	0.95	0.92
		RMS Focal Position Error (mm)	65.67			RMS Focal Position Error (mm)	34.66	26.33
		90% Focal Circle Radius (mm)	109.80			90% Focal Circle Radius (mm)	44.87	37.08
	Reflector 3	RMS Surface Error (mm)	0.92		Reflector 6	RMS Surface Error (mm)	0.43	0.51
		RMS Slope Error (mRadian)	32.00			RMS Slope Error (mRadian)	15.5	14.9
		Focus (m)	0.91			Focus (m)	0.99	0.95
		RMS Focal Position Error (mm)	63.37			RMS Focal Position Error (mm)	34.34	29.91
		90% Focal Circle Radius (mm)	108.53			90% Focal Circle Radius (mm)	50.90	48.48

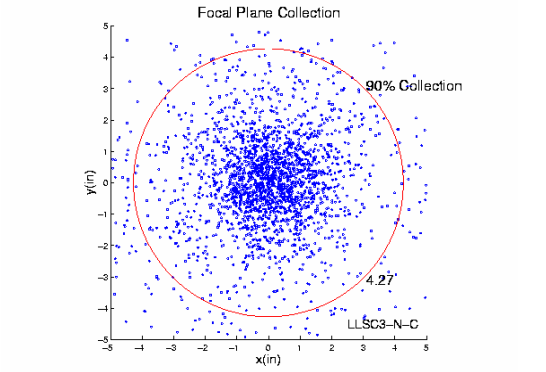

Figure 5. Typical Sub-T_g Reflector Collection Plot.

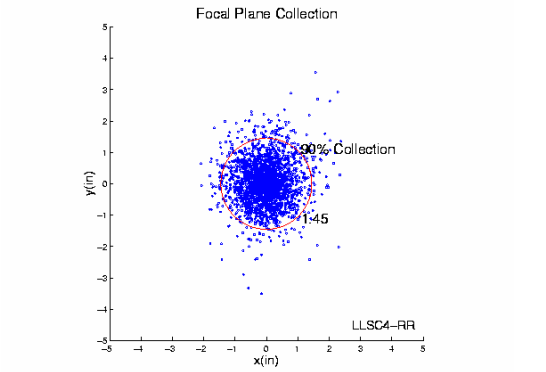

Figure 6. Typical Aluminum/Mylar Collection Plot.

B. 3-Meter Test Reflectors

Two 3-meter reflector test articles were fabricated using the aluminum/plastic laminate, which was chosen as the technology of choice for further development. The first test-article was fabricated for in-house testing. The second

test article was fabricated for testing at NASA Glenn Research Center's Tank 6 facility. Figure 7 shows a picture of one of the 3-meter reflectors mounted in the support structure for in-house testing.

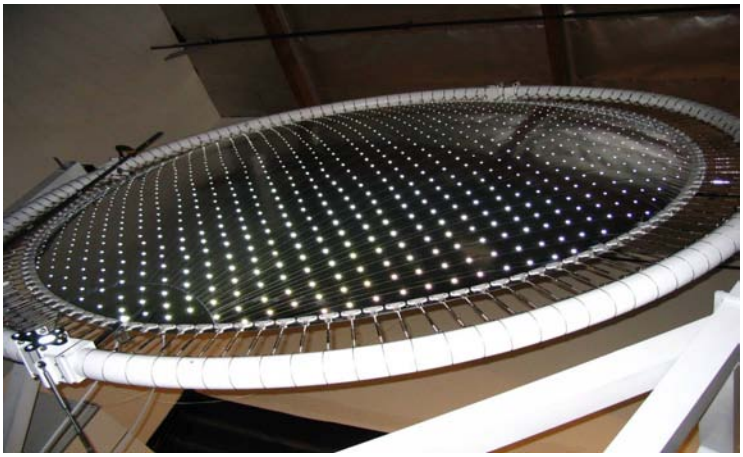

Figure 7. Rigidized 3-Meter Test Article Viewed from the Backside.

A summary of the 3-meter test article performance is included in Table 5. The best performance occurs when rigid and with the focal plane moved up by 7.75 in. As can be seen from Fig. 8 the focal dot is not much larger than the 5in. secondary collector.

Table 5. 3-Meter Test Article Results.

Test Condition	Focal Postion	Collection in a 5" Secondary	Radius of the 90% Collection Circle
Pressurized	y = 0	31%	10.4"
Rigid	y = 0	27%	8.4"
Rigid	y = 4.875"	45%	7.3"

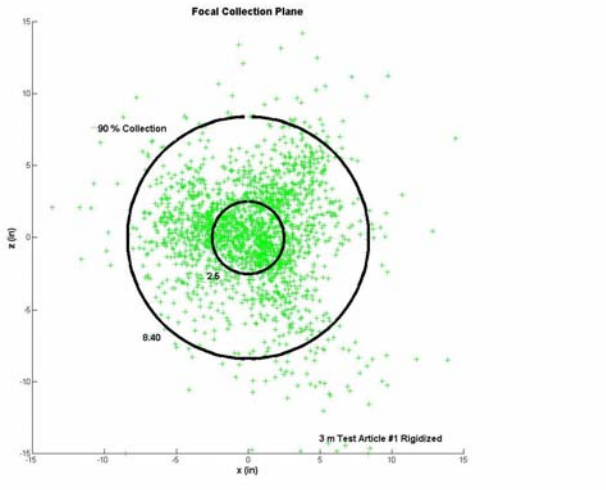

Figure 8. 3-Meter Test Reflector Collection Plot (Rigidized)

VII. Conclusion

The two rigidization techniques--cold rigidization and work hardening--were evaluated and thoroughly tested. Previous difficulties related to CTE in cold rigidization were overcome by creating a low-CTE cold-rigidizable composite. Also, much work was done in understanding the forming of the aluminum laminates, and an advanced laminate selection was created.

Three, 1-meter diameter aluminum-laminate reflectors were constructed, rigidized, and tested to measure the rigidized surface precisions with excellent results. Additionally, three 1-meter diameter cold-rigidizable reflectors were fabricated and tested at simulated space temperatures to test the composite improvements. The results of these tests were also favorable but not as good as the aluminum laminate.

To best advance the technology, the work hardening of an aluminum/plastic laminate was chosen as the best method and tested on a 3-meter test articles. Two 3-meter reflectors and a test fixture for NASA Glenn Research Center's Tank 6 facility were fabricated. Rigidization testing was done on one of the 3-meter reflectors, resulting in favorable concentration potential. The reflector held its shape under gravitational loading with no inflation pressure, and the focus was centered on the focal plane. Future work will be required to improve the concentration ratio, and will include more advance analyses of the material forming process.

Inflation-deployed rigidizable structures offer the advantages of low mass and stowed volume, high reliability, and low cost space structures that will significantly enhance America's space competitiveness. L'Garde's solar concentrator concept demonstrated these advantages through fabrication and testing of advanced prototype reflectors. The ability to lower the mass and volume of a space structure will be very attractive to satellite manufacturers, since this translates into lower launch costs. Currently, L'Garde is marketing the core technology advanced by this program for use in other applications, including optical and RF calibration objects.

Acknowledgments

The authors thank Mr. Wayne Wong of NASA Glenn Research Center for his support in the development of this technology. The authors also thank Dr. Costas Cassapakis and Mr. Gordon Veal for their vision, guidance, and pioneering work in the field of inflatable space structures.

References

[1]Lichodziejewski, D., and Cassapakis, C., "Inflatable Power Antenna Technology," AIAA 99-1074, 37th AIAA Aerospace Sciences Meeting and Exhibit, Reno, NV, Jan, 11-14, 1999.

[2]Cassapakis, C., and Thomas, M., "A Power Antenna for Deep Space Missions," Solar Engineering, ASME book No. H01046, 1996, pps. 435-441.

[3]Guidanean, K., and Veal, G., "An Inflatable Rigidizable Calibration Optical Sphere," AIAA 03-1899, 44th AIAA/ASME/ASCE/AHS/ASC Structures, Structural Dynamics, Materials Conference, Norfolk, Virginia, Apr. 7-10, 2003.

[4]Guidanean, K., Lichodziejewski, D., "An Inflatable Rigidizable Truss Structure Based on New Sub-T_g Polyurethane Composites, AIAA 02-1593, 43rd AIAA/ASME/ASCE/AHS/ASC Structures, Structural Dynamics, and Materials Conference, Denver, Colorado, Apr. 22-25, 2002.